Journal of Biomedical Optics

SPIEDigitalLibrary.org/jbo

Raman spectroscopy of normal oral buccal mucosa tissues: study on intact and incised biopsies

Atul Deshmukh
S. P. Singh
Pankaj Chaturvedi
C. Murali Krishna

SPIE

Raman spectroscopy of normal oral buccal mucosa tissues: study on intact and incised biopsies

Atul Deshmukh,[a,*] S. P. Singh,[a,*] Pankaj Chaturvedi,[b] and C. Murali Krishna[a]
[a]Chilakapati Laboratory, ACTREC, Kharghar, Navi-Mumbai, 410210
[b]Tata Memorial Hospital, Department of Surgical Oncology, Mumbai, 400012, India

Abstract. Oral squamous cell carcinoma is one of among the top 10 malignancies. Optical spectroscopy, including Raman, is being actively pursued as alternative/adjunct for cancer diagnosis. Earlier studies have demonstrated the feasibility of classifying normal, premalignant, and malignant oral *ex vivo* tissues. Spectral features showed predominance of lipids and proteins in normal and cancer conditions, respectively, which were attributed to membrane lipids and surface proteins. In view of recent developments in deep tissue Raman spectroscopy, we have recorded Raman spectra from superior and inferior surfaces of 10 normal oral tissues on intact, as well as incised, biopsies after separation of epithelium from connective tissue. Spectral variations and similarities among different groups were explored by unsupervised (principal component analysis) and supervised (linear discriminant analysis, factorial discriminant analysis) methodologies. Clusters of spectra from superior and inferior surfaces of intact tissues show a high overlap; whereas spectra from separated epithelium and connective tissue sections yielded clear clusters, though they also overlap on clusters of intact tissues. Spectra of all four groups of normal tissues gave exclusive clusters when tested against malignant spectra. Thus, this study demonstrates that spectra recorded from the superior surface of an intact tissue may have contributions from deeper layers but has no bearing from the classification of a malignant tissues point of view. *© 2011 Society of Photo-Optical Instrumentation Engineers (SPIE).* [DOI: 10.1117/1.3659680]

Keywords: Raman spectroscopy; oral cancers; principal component analysis; linear discriminant analysis, factorial discriminant analysis.

Paper 11284RR received Jun. 6, 2011; revised manuscript received Oct. 19, 2011; accepted for publication Oct. 20, 2011; published online Nov. 29, 2011.

1 Introduction

Oral mucous membrane, the epithelial lining of the oral cavity, is composed of stratified squamous epithelium. Oral squamous cell carcinoma, arising from epithelial lining, is the sixth most common malignancy worldwide. It accounts for more than 90% of the malignant tumors of oral cavity.[1] Tobacco chewing is one of the major factors responsible for malignant transformation of oral epithelium. All forms of tobacco-cigarettes, pipes, cigars, and smokeless tobacco have been implicated in the development of oral cancers. Incisional biopsy followed by histopathological examination is the current gold standard for diagnosis of oral squamous cell carcinoma. Traumatic and painful biopsy procedures, time consuming histopathological processing, and the interobserver variability in the diagnosis of potentially premalignant lesions, are some of the well-known drawbacks of conventional diagnosis.[2] Hence, there exists a need to explore alternative, noninvasive, atraumatic, and fast diagnostic tools which can exploit biochemical changes that occur during transformation of normal mucosa to premalignant and/or malignant lesions.

Optical spectroscopic methods are being pursued as alternatives or adjunct to existing diagnostic methods. A variety of optical-based techniques such as fluorescence; Raman and Fourier-transform infrared spectroscopy have been explored for development of newer diagnostic tools in oral cancers.[3–7] Among spectroscopic methods, Raman spectroscopy, which is based on inelastic scattering of photons, is an ideal tool, especially for *in vivo* applications. This is due to noninterference of water signals, information rich spectral features, and use of less harmful near-infrared excitations. Efficacy of Raman spectroscopy in classifying a variety of cancers under *ex vivo* and *in vivo* conditions has been demonstrated.[8–10]

We have earlier shown that Raman spectroscopy can be used for classifying normal, cancerous, and inflammatory conditions in oral tissues.[5–7] Recent studies have shown the feasibility of recording Raman spectra under *in vivo* conditions in clinically implementable time.[11,12] Major spectral features of both *ex vivo* and *in vivo* normal and malignant conditions show an abundance of lipids and proteins, respectively.[5–7] These spectral features have been corroborated by other groups also.[13] These features have been attributed to lipids and proteins of cell membranes. It is believed that Raman scattering from upper layers can reach more efficiently to detectors as compared to deeper layers owing to losses due to multiple scattering.[5–7,14–16] However, in view of recent developments in deep tissue Raman spectroscopy,[17] the origin of spectral features probably needs a relook. Hence, we have recorded Raman spectra of *ex vivo* normal oral tissues from epithelium (superior) and connective tissue (inferior) surfaces. Spectra were also recorded from the same surfaces of incised biopsies after separation of epithelium from connective tissue. Multivariate tools such as principal component analysis (PCA), linear discriminant analysis (LDA), and factorial discriminant analysis (FDA) were used for spectral analysis. A discussion on findings of the study has been reported in the paper.

*Contributed equally to this work.

Address all correspondence to: Chilakapati Murali Krishna, Chilakapati Laboratory, CRI ACTREC, TMC, Khargar, Navi Mumbai, Maharashtra 410210 India; Tel: 0091222740 5039; Fax: 00912227405085; E-mail: pittu1043@gmail.com

1083-3668/2011/16(12)/127004/10/$25.00 © 2011 SPIE

2 Materials and Methods

2.1 *Intact and Incised Biopsy Components*

Ten scalpel biopsies of approximately 8×6×5 mm dimensions from contralateral buccal mucosa of 10 oral cancer patients were collected. Tissue samples were collected in PBS saline and transferred to liquid nitrogen. Two frozen sections, each of 5-μm thickness, were cut longitudinally by orienting epithelium and connective tissue in order, which were used for histopathological examination. The remaining tissue was placed on a CaF_2 window and used for recording Raman spectra.

In the first step, Raman spectra from epithelium (superior surface of biopsy) referred to as "intact epithelium" and the connective tissue (inferior surface of biopsy) henceforth termed as "intact connective tissue," was recorded. A total of 68 and 53 spectra were recorded from intact epithelium and intact connective tissue, respectively.

In the second step, Raman spectra of the same surfaces of incised biopsies were recorded. In this case, epithelium was separated from connective tissues using surgical blade no.11 attached to a Bard–Parker handle. The procedure of biopsy and separation of an oral tissue component was followed as per the routine technique used in maxillofacial surgery practice.[18] Raman spectra from same surfaces (superior and inferior) were recorded. These two surfaces of the separated sections henceforth would be referred as "separated epithelium-upper" and "separated connective tissue-lower." A total of 54 and 59 spectra were recorded from these surfaces, respectively. A schematic representation of experimental protocol of spectral acquisition is shown in Fig. 1.

We have also recorded 128 spectra from 15 histopathologically confirmed tumor (oral squamous cell carcinoma) biopsies of buccal mucosa, collected from 15 subjects.

The use of human tissue biopsies was approved by the institutional ethical committee.

2.2 *Raman Spectroscopy*

On average, 5 to 6 spectra from 4 surfaces (intact epithelium, intact connective tissue, separated epithelium-upper, and separated connective tissue-lower) of 10 tissues were recorded using HE-785 commercial Raman spectrometer (Jobin-Vyon-Horiba, France). Briefly, this system consists of a diode laser (Process

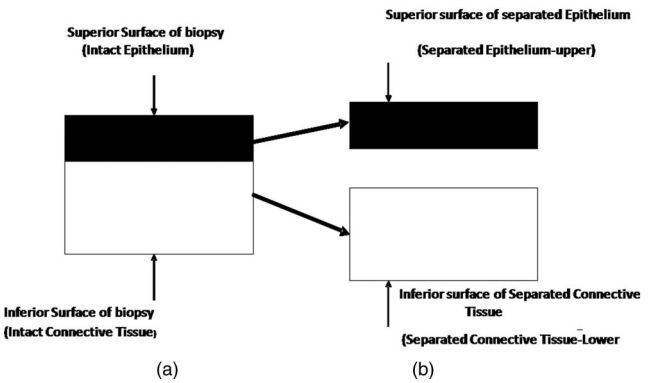

Fig. 1 Protocol of spectral acquisition: Schematic presentation: (a) intact tissue and (b) separated epithelium and connective tissue.

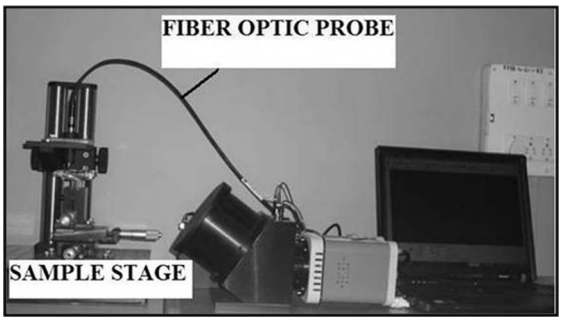

Fig. 2 Photographic representation of the Raman setup.

Instruments) of 785-nm wavelength as excitation source, a HE 785 spectrograph coupled with a CCD (Synapse) as dispersion, and detection elements. The spectrograph is equipped with a fixed 950 gr/mm and has no movable parts. Spectral resolution, as specified by the manufacturer, is ~4 cm^{-1}. Commercially available InPhotonics (Downy St., USA) probe consisting of 105 μm excitation fiber and 200 μm collection fiber (NA 0.40) was used to couple the excitation source and detection system. As per specifications of the manufacturer of the Inphotonics probe, the theoretical spot size and depth of field are 105 μm and 1 mm, respectively. Spectral acquisition parameters were: λ_{ex} 785 nm, laser power 80 mW, spectra were integrated for 10 s and averaged over 5 accumulations. Spectra were recorded with a spacing of ~2 mm using a manual *XYZ* precision stage. Photographic representation of the instrument is shown in Fig. 2.

3 Data Analysis

Preprocessed spectra from *ex vivo* tissues (corrected for CCD response and spectral contamination from CaF_2 background as well as from fibers) were first derivatized followed by vector normalization. Spectra in the 1200 to 1800 cm^{-1} region were then subjected to unsupervised, as well as supervised, discrimination analysis using an algorithm implemented in MATLAB-based in-house software.[19]

In the first step, unsupervised PCA of spectra from all four groups (intact epithelium, intact connective tissue, separated epithelium-upper, and separated connective tissue-lower) was performed. Different spectral ranges and factors were explored to bring out the best feasible classification. In our analysis, the spectral range of 1200 to 1800 cm^{-1} with 10 factors conferred the best results. In the next step, PCA was carried out on two different groups, i.e., intact epithelium, intact connective tissue, separated epithelium-upper, and separated connective tissue-lower. PCA of tumor spectra with all four groups of normal tissue were also performed. Loading of factors that were used for classification are shown in Figs. 3(a)–3(h). Supervised methods, i.e., LDA and FDA, were also employed to explore the feasibility of classification. Scree plots of LDA and FDA are shown in Figs. 3(i)–3(l).

4 Results and Discussion

Mean Raman spectra of intact epithelium, intact connective tissue, separated epithelium-upper, separated connective tissue -lower, and tumors in the 1200 to 1800 cm^{-1} region are shown

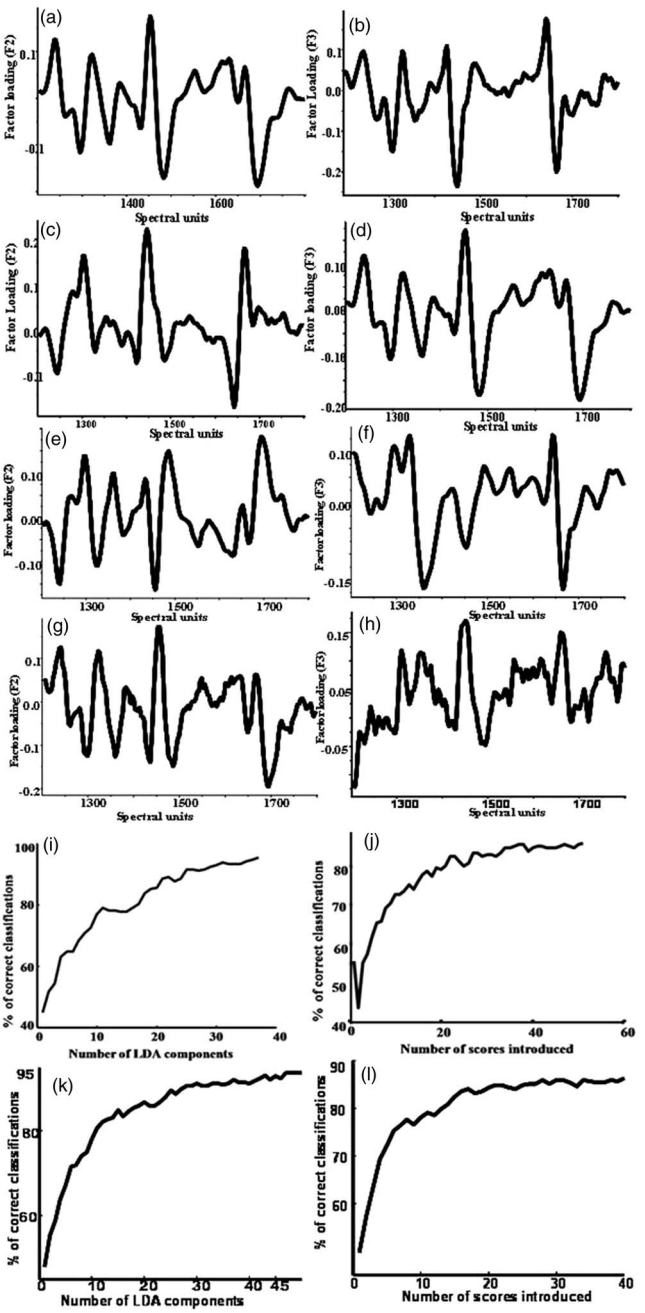

Fig. 3 Loadings of factor 2 and 3 used for PCA of intact tissues and separated sections [(a) and (b)]; intact tissues [(c) and (d); separated sections [(e) and (f)]; PCA along with tumor tissues and intact and incised biopsies [(g) and (h)]. Scree plots of LDA and FDA of intact and incised normal tissues [(i) and (j)] normal (intact and incised) and tumor tissues [(k) and (l)].

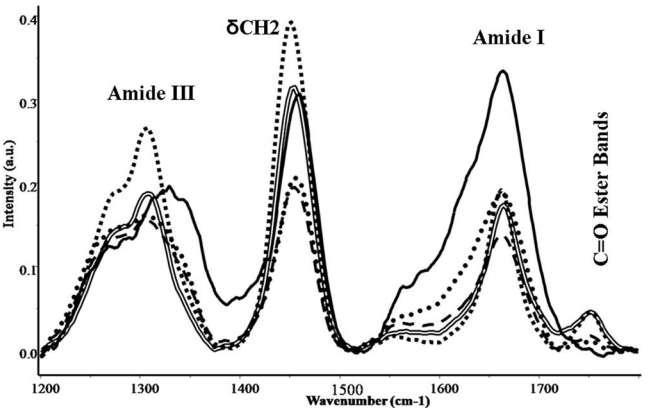

Fig. 4 Mean spectra of *ex vivo* oral tissues (round dots: intact epithelium; square dots: intact connective tissue; broken line: separated epithelium-upper; double line: separated connective tissue-lower; solid line: tumor).

in Fig. 4. Spectral features of normal tissues are suggestive of predominant lipid signatures indicated by ester bands, strong δCH_2 bend, two sharp features around amide III, and a sharp peak around amide I. Dominating protein features indicated by broad amide III, broadened δCH_2, and broad features in the amide I region were seen in the mean tumor spectrum. These features substantiate earlier *ex vivo* and *in vivo* studies.[5–7, 10, 12] Spectra of intact and separated connective tissue show strong lipid features as compared to spectra from epithelial surfaces. Likewise, spectra of intact and separated epithelium are similar. In this case, additional broad features in amide III and amide I regions can also be seen. To understand heterogeneity among spectral features, mean and standard deviation spectra of all five groups were computed. As shown in Figs. 5(a)–5(e), major heterogeneities in the spectra were observed which can be attributed to variations in lipid and protein components indicated by amide III, amide I and C=O stretching of ester bands. As a whole, after considering spectral variations shown in standard deviations, probably spectra of all four groups of normal tissues share several common features.

To understand the above-mentioned variations and similarities across the spectra of different classes and to explore the feasibility of classification, data analysis by unsupervised (PCA) and supervised (LDA, FDA) multivariate methods was taken up. PCA was performed in two steps. In the first stage, PCA of data from all four groups (intact epithelium, intact connective tissue, separated epithelium-upper, and separated connective tissue-lower) was carried out. The loading plots of factors 2 and 3, which were explored for classification, are shown in Figs. 3(a) and 3(b). No clear classification was observed. The results obtained in our analysis are shown in Fig. 6(a), wherein spectra from intact tissues (intact epithelium and intact connective tissue) gave highly overlapping clusters, while spectra from separated epithelium-upper and separated connective tissue-lower showed a tendency of classification, although they overlapped with clusters of intact tissues. In the next step, spectral data of intact epithelium, intact connective tissue, separated epithelium-upper, and separated connective tissue-lower were subjected to PCA in two different groups [Figs. 6(b) and 6(c)]. Once again, no classification could be achieved among spectra of intact tissues (intact epithelium and intact connective tissue). The typical results of spectral analysis are shown in Fig. 6(b). Loading plots of factors 2 and 3 which were used for classification are shown in Figs. 3(c) and 3(d). Conversely, PCA of the second group, i.e., separated sections gave a clean classification as shown in Fig. 6(c). In this case, once again factors 2 and 3 were used for classification and loading plots of which are shown in Figs. 3(e) and 3(f). These results probably suggest that spectral differences across intact tissues (intact

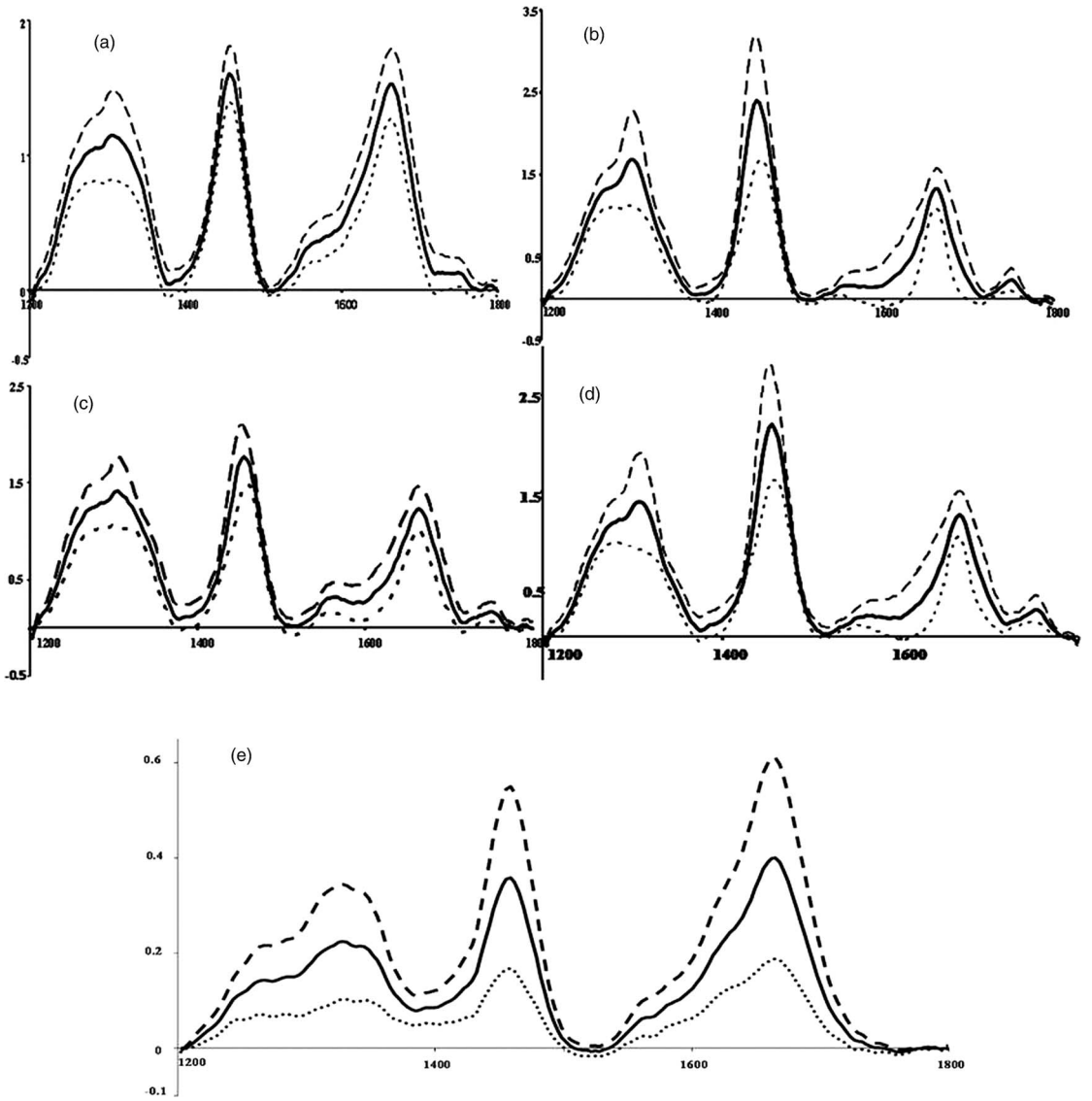

Fig. 5 Mean and standard deviation spectra: (a) intact epithelium, (b) intact connective tissue, (c) separated epithelium-upper, (d) separated connective tissue-lower, and (e) tumor. (Solid line: mean spectra; broken line: positive standard deviation; dotted line: negative standard deviation.)

epithelium and intact connective tissue) are minimal as compared to that of separated sections (separated epithelium-upper and separated connective tissue-lower). However, a point to be noted is that PCA is considered more as a data overview tool rather than a classification methodology; it gives a sketch out of the data, which in turn reveals outliers, groups, and trends in the data.[20]

Therefore, we have also explored possible discrimination among four groups by supervised methods (LDA, FDA). Significant principal components ($P < 0.05$) were selected as input for the development of LDA algorithms. LDA determines the discriminant function that maximizes the variances in the data between groups while minimizing the variances between members of the same group. Factors up to 95% variances were used [Fig. 3(i)]. The performance of the diagnostic algorithms rendered by the LDA models for correctly predicting the tissue groups was estimated in an unbiased manner using the leave-one-out (LOO) cross-validation method. As shown in Fig. 7, four clusters—each corresponding to intact epithelium, intact connective tissue, separated epithelium-upper, and separated connective tissue-lower, respectively—were obtained. Further analysis of the scatter plot (Fig. 7) suggests that clusters corresponding to intact epithelium and intact connective tissue are more closer, while clusters of separated epithelium-upper and separated connective tissue-lower are placed far apart from each other. A summary of classifications for all groups is shown in Table 1. Sixty-five out of 68 spectra of intact epithelium and 50 out of 53 spectra of intact connective tissue 52 out of 54 spectra of separated epithelium-upper and 55 out of 59 spectra of separated connective tissue-lower were correctly classified. Overall, a classification efficiency of 94% was observed.

LOO is a cross-validation method used for evaluation of a performance of the classification models without losing diversity in the data. Findings of LOO are shown in Table 1 which suggests large misclassification across different groups. The confusion matrix indicates that intact tissues are showing most of the misclassifications. Out of 16 misclassifications of intact epithelium spectra, 10 are classified as separated epithelium-upper, 2

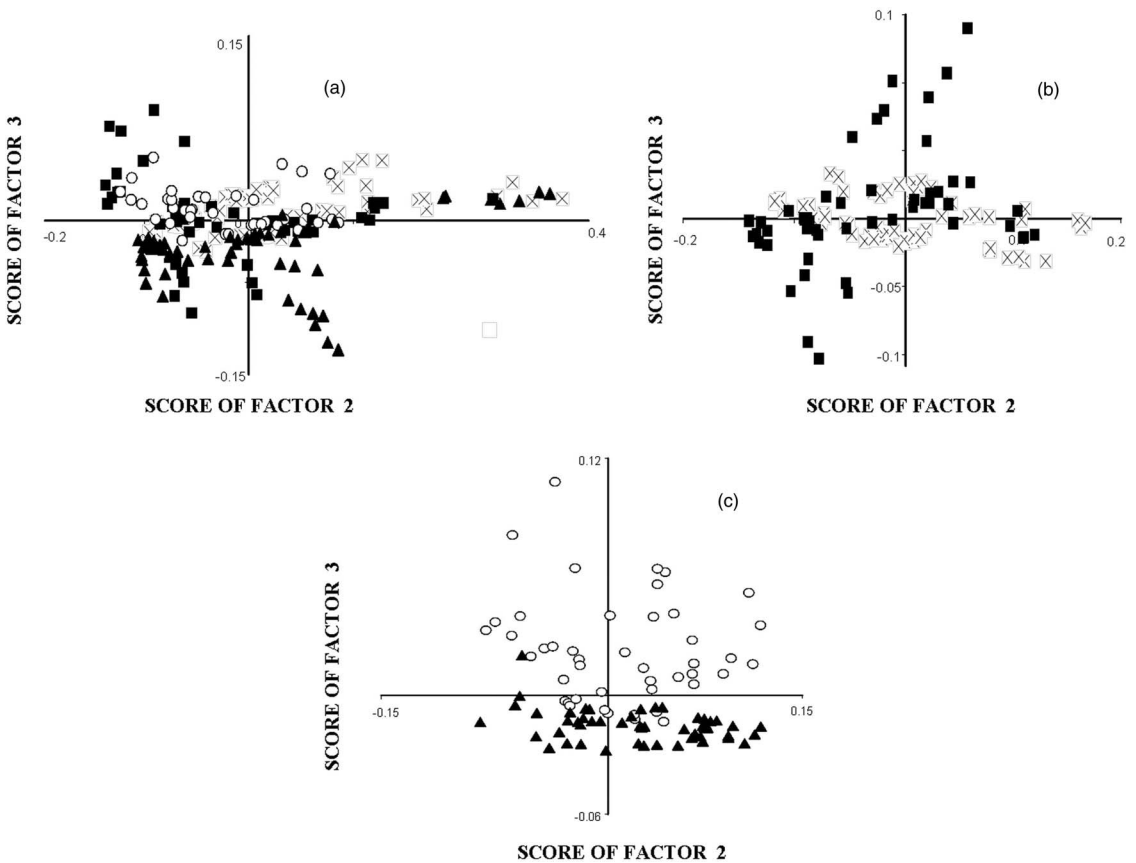

Fig. 6 PCA of oral spectra: (a) intact and incised biopsies; (b) intact tissues; (c) incised tissue (×: intact epithelium, ■: intact connective tissue, o: separated epithelium-upper; ▲: separated connective tissue-lower).

as intact connective tissue, and 4 as separated connective tissue-lower. Twenty-one misclassifications were observed in the case of intact connective tissue spectra out of which 9, 4, and 8 spectra were classified as intact epithelium, separated epithelium-upper, and separated connective tissue-lower, respectively. But the situation is different when the spectra of separated sections were considered. In this case, most of the spectra overlap with intact tissues, e.g., out of 25 misclassifications of separated epithelium-upper only 4 are misclassified as separated connective tissue-lower group. Similarly, only 2 out of 16 spectra of separated connective tissue-lower group were misclassified as separated epithelium-upper. Twenty-one and 14 misclassifications of spectra from separated epithelium-upper and separated connective tissue-lower were intact epithelium and intact connective tissue, respectively. It could be due to the fact that spectral features of intact tissues might have signals from both epithelium and connective tissue components, thus supporting the findings of PCA (Fig. 6).

Further, FDA was employed to verify findings of PCA and LDA among different groups. FDA is an extremely useful whenever there are grounds to postulate the existence of a number of groups (categories) into which the samples may be classified, and one has to look for the best discrimination. In this approach, sample cases are attributed to the group on the basis of classification probability of each spectrum, computed from the distance in discriminant space of PCA scores between the spectrum and the centroid of the nearest class. FDA aims to find a small number of generalized variables (or factors) that can describe most of the variances and correlations of the initial variables (in this case, Raman shift wave number), reducing the dimension of the measurement space without loss of information. Factors accounting for up to 80% variance were used for analysis [Fig. 3(j)]. As can be seen in Fig. 8, in this case and as observed in PCA and LDA (Figs. 6 and 7, and Table 1), spectra belonging to intact tissues show an overlap among themselves and also with separated sections. But spectra from separated sections are very exclusive.

As mentioned earlier, efficacy of Raman spectroscopy in classifying normal, malignant, and premalignant conditions has already been demonstrated.[5–7] But in these studies Raman spectra were recorded on intact tissues. Therefore, we have analyzed spectra of tumor tissues along with spectra from all four different groups (intact and incised oral normal biopsies) by PCA, LDA, and FDA. Loading plots of factor 2 and 3 used for PCA and scree plots for LDA and FDA are shown in Figs. 3(g) and 3(h) and Figs. 3(k) and 3(l), respectively. Findings of PCA, LDA, and FDA are shown in Figs. 9(a)–9(c) and Table 2, respectively, which indicate that tumor spectra are always exclusive and do not overlap with any of the four groups of normal spectra. It also indicates that surface, i.e., orientation of normal tissues, seems to have no bearing on classification.

Buccal mucosa is the nonkeratinized membrane lining of the oral cavity. Oral buccal mucosa contains epithelium (superficial portion), lamina propria (subepithelial connective tissue), and submucosa (deeper portion of connective tissue containing adipose and muscle tissue). Oral epithelium is of stratified

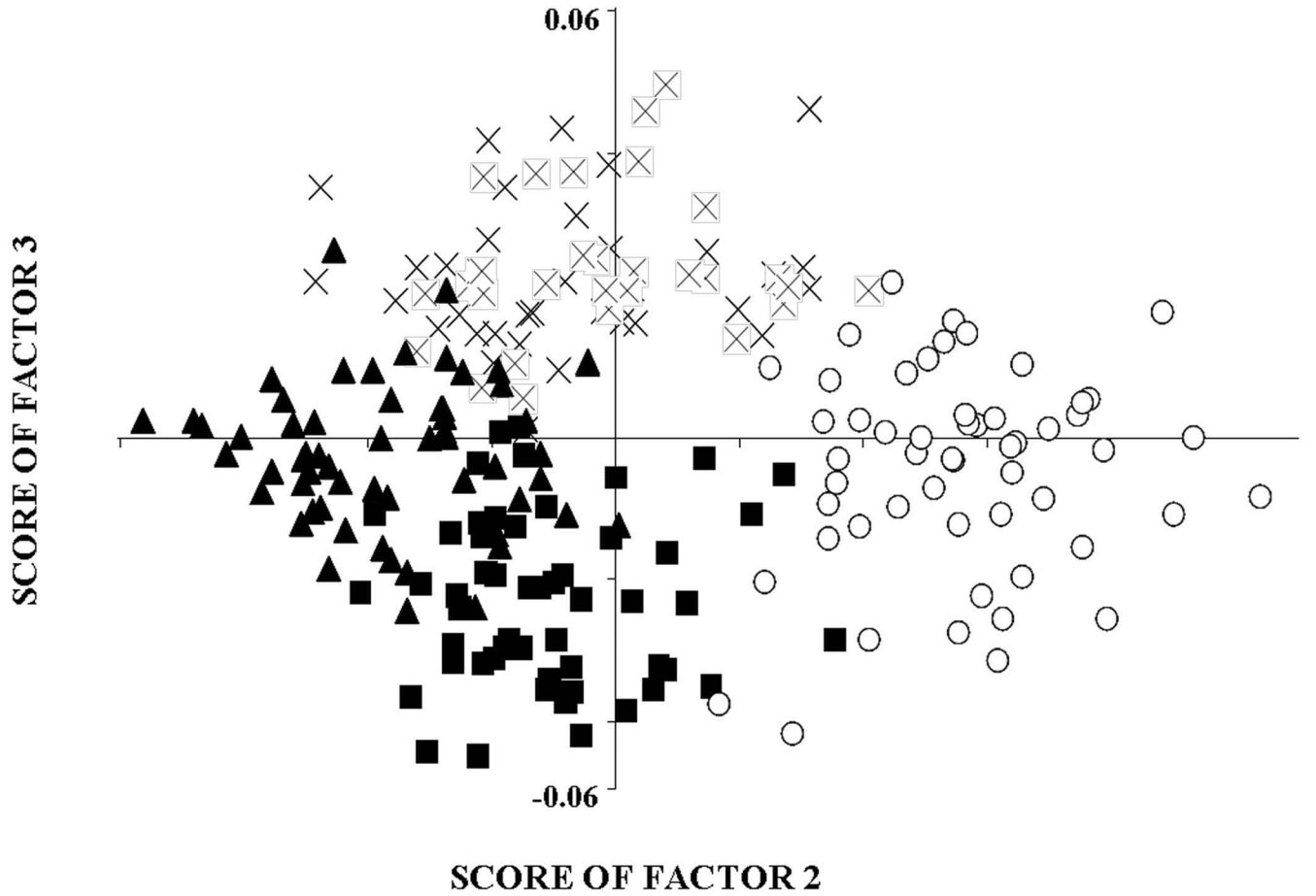

Fig. 7 LDA of spectra from intact and incised biopsies (×: intact epithelium; ■: intact connective tissue; o: separated epithelium-upper; ▲: separated connective tissue-lower).

squamous type. The connective tissue of oral mucosa is called lamina propria. It is supported by submucosa which is attached to the underlying periosteum and bone through muscles. Epithelial stratification shows three layers, basal cell layer (stratum basalis), prickle cell layer (stratum spinosum), and corneal cell layer (stratum corneum). Thickness of oral epithelium is variable according to the site. Epithelium of buccal mucosa is the thickest of all oral epithelia, which is approximately 500 μm. Epithelium and connective tissues are separated by a 1 to 2-μm thick structureless layer called a basement membrane. Lamina propria contains reticulin and collagen fibers. Submucosa of oral mucosa shows adipose tissue and minor salivary gland acini.[21] A schematic representation of normal buccal mucosa is shown in Fig. 10(a).

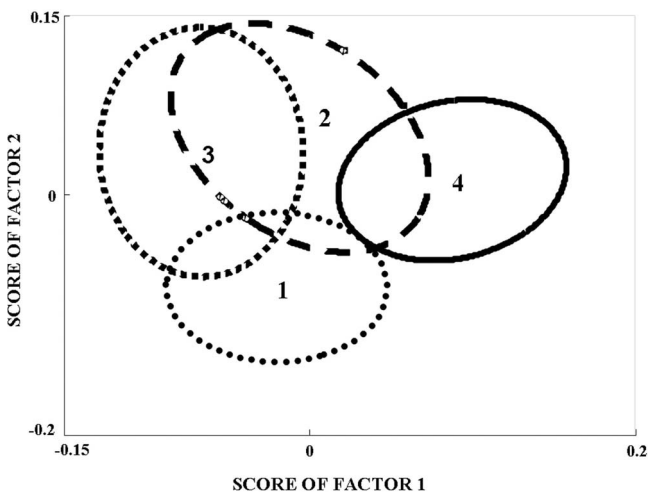

Fig. 8 FDA of spectra from intact and incised biopsies (1: intact epithelium, 2: intact connective tissue; 3: separated epithelium-upper; 4: separated connective tissue-lower).

In the present experiments, tissue samples were collected from contralateral normal buccal mucosa of oral cancer subjects. Histopathological representation of a typical oral normal buccal mucosa tissue used in the study is shown in Fig. 10(b). The average thickness of the biopsies collected was ~5 mm. As mentioned earlier, the thickness of epithelium of buccal mucosa is ~0.5 mm and the rest of the thickness is due to reticulin and collagen fibers of lamina propria, adipose tissue, and minor mucous salivary glands of submucosa and ground substance of connective tissue.[21] In the first step spectra were recorded from superior and inferior surfaces of intact biopsy samples [Fig. 10(b)]. As per the specifications given by the manufacturer, the depth of field of the probe is 1 mm. When spectra were recorded from a superior surface of the biopsy, we presume that the entire buccal epithelium, lamina propria, and a portion of the submucosal adipose tissue have contributed to the spectrum. It may be the reason for Raman signals of lipids and proteins

Table 1 Confusion matrix: analysis of intact and incised oral normal buccal mucosa spectra. (Diagonal elements are true positive predictions and Ex-diagonal elements are false positive predictions.)

LDA	Intact epithelium	Intact connective tissue	Separated epithelium-upper	Separated connective tissue-lower
Intact epithelium	65	1	2	0
Intact connective tissue	2	50	1	0
Separated epithelium-upper	0	2	52	0
Separated connective tissue-lower	1	3	0	55
LDA Leave-one-out cross-validation	**Intact epithelium**	**Intact connective tissue**	**Separated epithelium-upper**	**Separated connective tissue-lower**
Intact epithelium	52	2	10	4
Intact connective tissue	9	32	4	8
Separated epithelium-upper	10	11	29	4
Separated connective tissue-lower	7	7	2	43
FDA	**Intact epithelium**	**Intact connective tissue**	**Separated epithelium-upper**	**Separated connective tissue-lower**
Intact epithelium	64	2	2	0
Intact connective tissue	4	43	4	2
Separated epithelium-upper	6	7	41	0
Separated connective tissue-lower	2	2	2	53

observed in the spectra. When Raman spectra were recorded from an inferior surface, a major contribution could be from adipose tissue of submucosa and a deeper collagenous zone of lamina propria. Also the possibility of contribution from the epithelial surface cannot be completely ruled out. This is more evident from Raman spectra showing strong lipid features along with protein features obtained from the inferior surface of a biopsy (Fig. 4). Strong lipid features could be attributed to the fact that the submucosal adipose tissue zone falls within the depth of field of the probe and the Raman cross-section of lipids is larger.[22,23] This is further supported by PCA, LDA, and FDA, wherein spectra belonging to superior and inferior surfaces of intact biopsies show a considerable overlap suggesting similarities in spectral profiles [Figs. 6(a)–8].

In the next step, epithelium was separated from the underlying connective tissue using a surgical blade and spectra were recorded from separated epithelium– upper and separated connective tissue–lower. As shown in Figs. 10(c), it is possible to separate epithelium from connective tissue without intermixing different layers. Spectra recorded from separated epithelium–upper seems to be different from separated connective tissue–lower which is composed of submucosal adipose tissue and collagen zone of lamina propria [Fig. 10(c)], especially in terms of strong lipid features seen in the latter. This is also evident from PCA, LDA, and FDA as clusters belonging to separated epithelium– upper and separated connective tissue–lower are mutually exclusive, however they overlap with intact tissue which further supports our observation that spectra from intact tissue have contributions from not only superficial layers but also from deeper layers [Figs. 6(a)–8].

From the findings of our study one can assume that architectural and morphological organization of tissue components are the hallmark of spectral signatures. Spectra obtained from upper and lower surfaces of an intact oral buccal mucosal biopsy showed lipid and protein signatures due to histological arrangement of lipid and collagen molecules in the connective tissue. On the other hand, spectra from the same surfaces after epithelium separation seem to be different but they overlap with intact tissue spectra as suggested by PCA, LDA, and FDA. Clusters of intact tissues overlap among themselves while clusters from separated sections remain exclusive. Therefore, it can be assumed that spectra recorded from either surface will have features from an entire volume of the probing area. This is probably due to a collection of signals even from deeper layers of tissue. There have been reports on propagation of Raman photons from deeper tissue layers.[24,25] A recent study by Mo et al. on a two layer tissue phantom constructed by overlaying different thicknesses of chicken muscle tissues on chicken fat tissue has demonstrated that spectral contributions of fat layers as deep as 3.9 mm can be recorded.[24] Our study also suggests that spectral

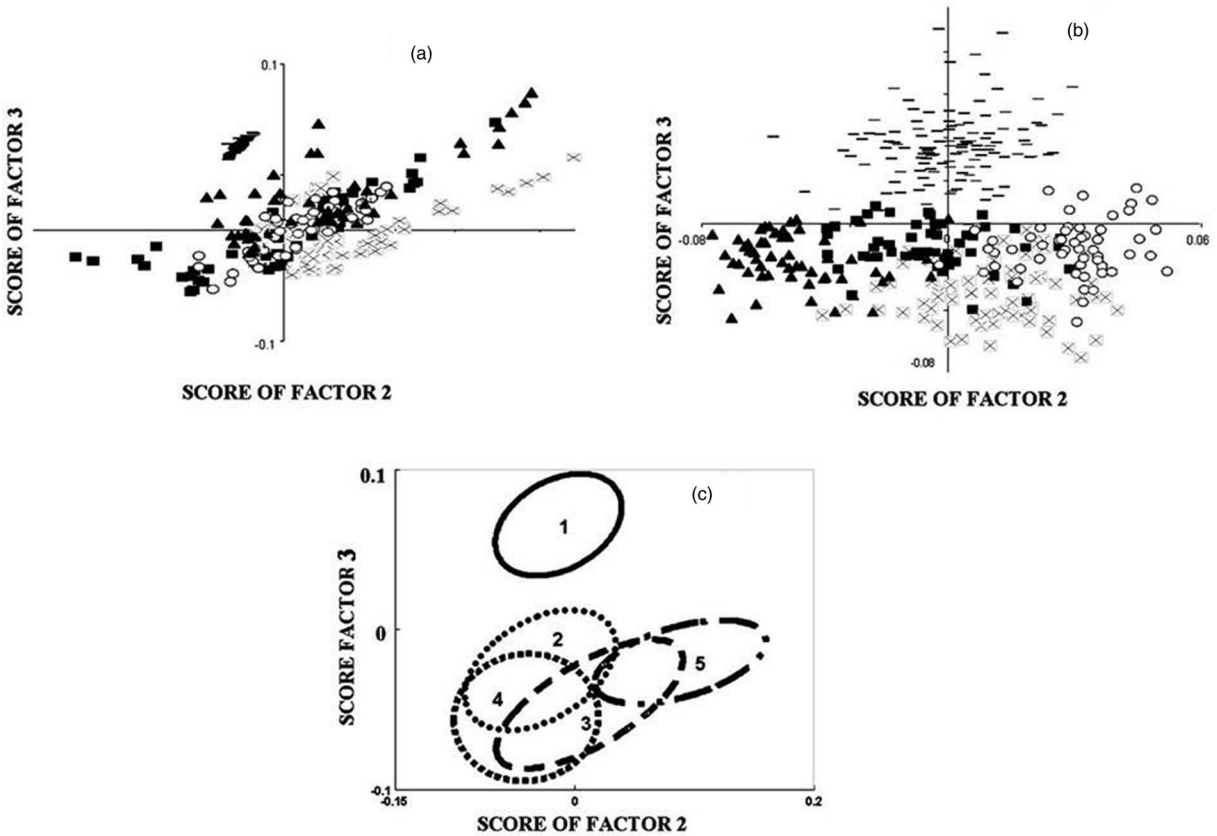

Fig. 9 Analysis of oral buccal normal and tumor spectra: (a) PCA, (b) LDA (×: intact epithelium; ■: intact connective tissue; o: separated epithelium-upper; ▲: separated connective tissue-lower, –: tumor). (c) FDA of oral buccal normal and tumor spectra (1: tumor; 2: intact epithelium; 3: intact connective tissue; 4: separated epithelium-upper; 5: separated connective tissue-lower).

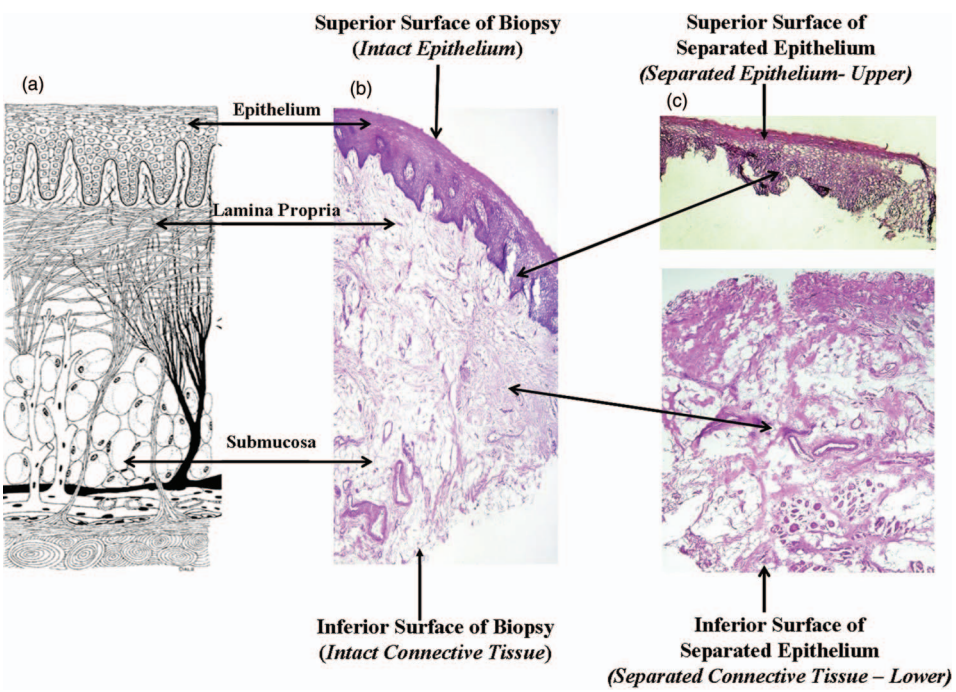

Fig. 10 Histological sections of buccal mucosa: (a) Schematic representation; (b) intact biopsy section; (c) separated components; epithelium–upper image, connective tissue–lower image.

Table 2 Confusion matrix: analysis of oral normal buccal mucosa and tumor spectra. (Diagonal elements are true positive predictions and Ex-diagonal elements are false positive predictions.)

LDA	Tumor	Intact epithelium	Intact connective tissue	Separated epithelium-upper	Separated connective tissue-lower
Tumor	127	0	1	0	0
Intact epithelium	0	65	1	2	0
Intact connective tissue	0	2	50	1	0
Separated epithelium-upper	0	0	2	52	0
Separated connective tissue-lower	0	1	3	0	55
LDA Leave-one-out cross-validation	**Tumor**	**Intact epithelium**	**Intact connective tissue**	**Separated epithelium-upper**	**Separated connective tissue-lower**
Tumor	116	3	5	2	2
Intact epithelium	0	51	3	9	5
Intact connective tissue	0	13	28	6	6
Separated epithelium-upper	0	12	12	28	2
Separated connective tissue-lower	0	4	3	2	50
FDA	**Tumor**	**Intact epithelium**	**Intact connective tissue**	**Separated epithelium-upper**	**Separated connective tissue-lower**
Tumor	127	0	1	0	0
Intact epithelium	0	63	0	4	1
Intact connective tissue	0	6	37	6	4
Separated epithelium-upper	0	6	8	40	0
Separated connective tissue-lower	0	2	2	1	54

contributions from deeper submucosal adipose tissue can be observed in spectra that we recorded from a superior surface of an intact tissue. PCA, LDA, and FDA findings also support this observation as spectra from superior and inferior surfaces show an overlap. However, surface orientations of normal tissue seem to have no influence on classification between normal and malignant tissues.

Considering *in vivo* applications, the present observation is very significant as morphological alterations in premalignant pathosis occur at the basal cell region which is ~300 to 400 μm deep from surface. If we assume that spectra would arise only from superficial layers, it would be difficult to diagnose potentially precancerous and early invasive lesions. The present experiment suggests that spectra arise from interaction of both epithelial and connective tissue components; hence, by achieving suitable modification in probe, confocal measurements can be made by targeting an area of specific interest.

Acknowledgments

This work was carried out under Project No. BT/PRI11282/MED/32/83/2008, Department of Biotechnology, and Government of India. The authors would like to acknowledge Ms. Arti R. Hole for help with the histopathological analysis of tissues.

References

1. D. M. Parkin, F. Bray, J. Fertay, and P. Pisani, "Global cancer statistics, 2002," *Ca-Cancer J. Clin.* **55**(2), 74–108 (2005).

2. L. M Abbey, G. E. Kaugars, J. C. Gunsolley, J. C. Burns, D. G. Page, J. A. Svirsky, E. Eisenberg, D. J. Krutchkoff, and M. Cushing, "Intraexaminer and interexaminer reliability in the diagnosis of oral epithelial dysplasia," *Oral Surg. Oral Med. Oral Pathol. Oral Radiol. Endod.* **80**(2), 188–191 (1995).
3. D. C. De Veld, M. J. Witjes, H. J. Sterenborg, and J. L. Roodenburg, "The status of *in vivo* autofluorescence spectroscopy and imaging for oral oncology," *Oral Oncol.* **41**(2), 117–131 (2005).
4. J. G. Wu, Y. Z Xu, C. W. Sun, R. D. Soloway, D. F. Xu, Q. G. Wu, K. H. Sun, S. F. Weng, and G. X. Xu, "Distinguishing malignant from normal oral tissues using FTIR fiber-optic techniques," *Biopolymers* **62**(4), 185–192 (2001).
5. K. Venkatakrishna, J. Kurien, K. M. Pai, C. Murali Krishna, G. Ullas, and V. B. Kartha, "Optical pathology of oral tissue: A Raman spectroscopy diagnostic method," *Curr. Sci.* **80**(1), 665–669 (2001).
6. C. M. Krishna, G. D. Sockalingum, J. Kurien, L. Rao, L. Venteo, M. Pluot, M. Manfait, and V. B. Kartha, "Micro-Raman spectroscopy for optical pathology of oral squamous cell carcinoma," *Appl. Spectrosc.* **58**(9), 1128–1135 (2004).
7. R. Malini, K. Venkatakrishna, J. Kurien, K. M. Pai, L. Rao, V. B. Kartha, and C. M. Krishna, "Discrimination of normal, inflammatory premalignant, and malignant oral tissue: a Raman spectroscopy study," *Biopolymers* **81**(3), 179–193 (2006).
8. A. Nijssen, S. Koljenovic, T. C. B. Schut, P. J. Caspers, and G. J. Pupples, "Towards oncological application of Raman spectroscopy," *J. Biophoton.* **2**(1-2), 29–36 (2009).
9. C. Kendall, M. Isabelle, F. B. Hegemark, J. Hutchings, and L. Orr, "Vibrational spectroscopy: a clinical tool for cancer diagnosis," *Analyst* **134**, 1029–1045 (2009).
10. V. B. Kartha, J. Kurien, L. Rai, K. K. Mahato, C. Murali Krishna, and C. Santhosh, "Diagnosis at the molecular level: Analytical laser spectroscopy for clinical applications," in *Photo/Electrochemistry & Photobiology in the Environment, Energy and Fuel*, pp. 153–221, Research Signpost, India (2005).
11. K. Guze, M. Short, S. Sonis, N. Karimbux, J. Chan, and H. Zeng, "Parameters defining the potential applicability of Raman spectroscopy as a diagnostic tool for oral disease," *J. Biomed. Opt.* **14**(1), 014016 (2009).
12. S. P. Singh, A. Deshmukh, P. Chaturvedi, and C. Murali Krishna, "Raman spectroscopy in head and neck cancers: towards oncological applications" *J. Cancer Res. Ther.* (2011) (in press).
13. Z. Huang, S. K. Teh, W. Zheng, J. Mo, K. Lin, X. Shao, K. Y. Ho, M. Teh, and K. G. Yeoh, "Integrated Raman spectroscopy and trimodal wide-field imaging techniques for real-time *in vivo* tissue Raman measurements at endoscopy," *Opt. Lett.* **34**(6), 758–760 (2009).
14. C. Murali Krishna, N. B. Prathima, B. M. Vadhiraja, R. Malini, D. J. Fernandes, M. S. Vidyasagar, and V. B. Kartha, "Raman spectroscopy studies for diagnosis of cancer in human uterine cervix," *Vib. Spectrosc.* **41**, 136–141 (2006).
15. C. M. Krishna, V. B. Kartha, R. Malini, K. Venkatakrishna, A. Agarwal, K. M. Pai, B. S. Thomas, L. Rao, M. Alexander, and J. Kurien, in *Biopolymer Research Trends*, T. S. Nemeth, Eds., pp. 189–209, Nova Science Publishers, Happauge, NY (2007).
16. A. T. Harris, A. Rennie, H. Waqar-Uddin, S. R. Wheatley, S. K. Ghosh, D. P. Martin-Hirsch, S. E. Fisher, A. S. High, J. Kirkham, and T. Upile, "Raman spectroscopy in head and neck cancer," *Head & Neck Oncol.* **2**(26), 1–6 (2010).
17. P. Matousek and N. Stone, "Emerging concepts in deep Raman spectroscopy of biological tissue," *Analyst* **134**(6), 1058–1066 (2009).
18. M. Michael, G. E. Ghall, P. E. Larsen, and P. D. Walte, *Peterson's Principles of Oral & Maxillofacial Surgery*, 2nd Ed., Decker, Inc., Hamilton, London (2004).
19. A. D. Ghanate, S. Kothiwale, S. P. Singh, D. Bertrand, and C. Murali Krishna, "Comparative evaluation of spectroscopic models using different multivariate statistical tools in a multicancer scenario," *J. Biomed. Opt.* **16**(2), 025003 (2011).
20. R. Madsen, T. Rundstedt, and J. Trygg, "Chemometrics in metabolomics-A review in human disease diagnosis," *Anal. Chim. Acta*, **659**(1–2), 23–33 (2010).
21. A. Nancy, *Tencate's Oral Histology: Development, Structure and Function*, Chap. 12, Mosby, Inc., an affiliate of Elsevier Inc., St. Louis, MO (2006).
22. A. S. Haka, K. E. Shafer-Peltier, M. Fitzmaurice, J. Crowe, R. R. Dasari, and M. S. Feld, "Diagnosing breast cancer by using Raman spectroscopy," *Proc. Natl. Acad.Sci. U.S.A.* **102**, 12371–12376 (2005).
23. C. M. Krishna, J. Kurien, S. Mathew, L. Rao, K. Maheedhar, K. K. Kumar, and M. V. Chowdary, "Raman spectroscopy of breast tissues," *Expert Rev. Mol. Diagn.* **8**(2), 149–66 (2008).
24. J. Mo, W. Zheng, and Z. Huang, "Fiber-optic Raman probe couples ball lens for depth-selected Raman measurements of epithelial tissue," *Biomed. Opt. Express* **1**(1), 7–30 (2010).
25. Y. S. Yamamoto, Y. Oshima, H. Shinzawa, T. Katagiri, and Y. Matsuura, "Subsurface sensing of biomedical tissues using a miniaturized Raman probe: Study of thin-layered model samples," *Anal. Chim. Acta* **619**, 8–13 (2008).